Electronic Supplementary Information

Novel Defect-Fluorite Pyrochlore Sodium Niobate Nanoparticles: Solution-Phase Synthesis and Radiation Tolerance Analysis

Rana Faryad Ali[†], Jeffrey S. Ovens[†], Krzysztof Starosta[†], Byron D. Gates[†,]*

[†] Department of Chemistry and 4D LABS, Simon Fraser University, 8888 University Drive Burnaby, BC, V5A 1S6, Canada

[*] E-mail: bgates@sfu.ca

This work was supported in part by the Natural Sciences and Engineering Research Council (NSERC) of Canada (Discovery Grant No. 1077758), and through the Collaborative Health Research Projects (CHRP) Partnership Program supported in part by the Canadian Institutes of Health Research (Grant No. 134742) and the Natural Science Engineering Research Council of Canada (Grant No. CHRP 462260), the Canada Research Chairs Program (B.D. Gates, Grant No. 950-215846), and CMC Microsystems (MNT Grant No. 4279). This work made use of 4D LABS (www.4dlabs.com) and the Center for Soft Materials shared facilities supported by the Canada Foundation for Innovation (CFI), British Columbia Knowledge Development Fund (BCKDF), Western Economic Diversification Canada, and Simon Fraser University. We also thank Dr. Rajendra Sharma for assistance with acquiring the data associated with the thermogravimetric analysis, and Professor Vance Williams and Carson Zellman for helping to acquire the data associated with the differential scanning calorimetry.

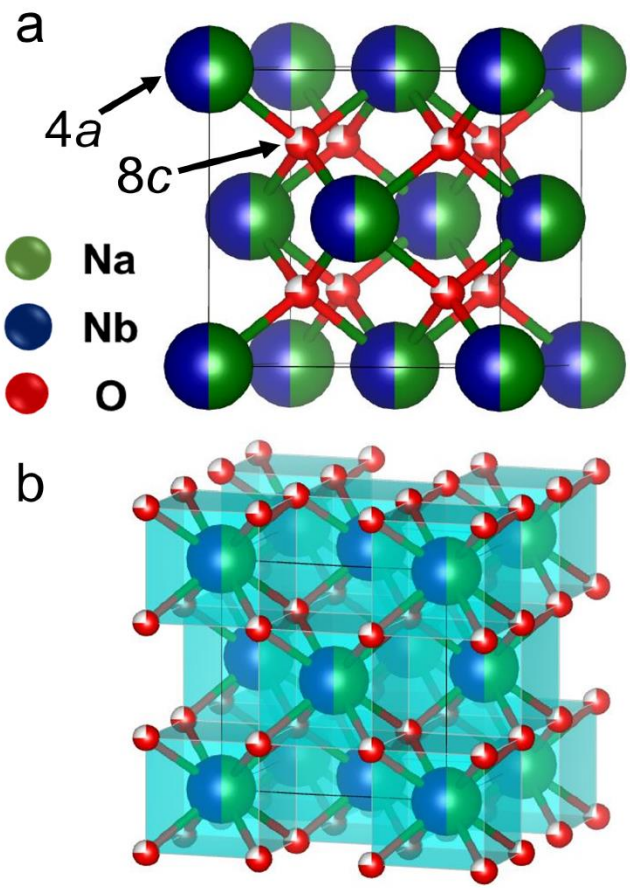

Fig. S1 A defect-fluorite or disordered pyrochlore structure with a corresponding formula of ABO_3. These structures show: (a) Na (e.g., A cation) and Nb (e.g., B cation) in a cubic $Fm\bar{3}m$ unit cell; and (b) polyhedra representing the local coordination environment around the Na and Nb cations.

Table S1. Rietveld refinement parameters for the crystal structure of pyrochlore sodium niobate ($NaNbO_3$) nanoparticles.

empirical formula	$NaNbO_3$
formula weight ($g \cdot mol^{-1}$)	163.89
crystal system	cubic
space group	$Fm\bar{3}m$
a (Å)	5.137(4)
b (Å)	5.137(4)
c (Å)	5.137(4)
α (deg.)	90
β (deg.)	90
γ (deg.)	90
V ($Å^3$)	135.0(3)
Z	1
T (K)	293(2)
ρ_{cal} ($g.cm^{-3}$)	4.013
$2\theta_{min}$, $2\theta_{max}$ (deg.)	10, 80
R_{exp}	0.0344
R_p, wR_p	0.0373, 0.0467
goodness of fit	1.00

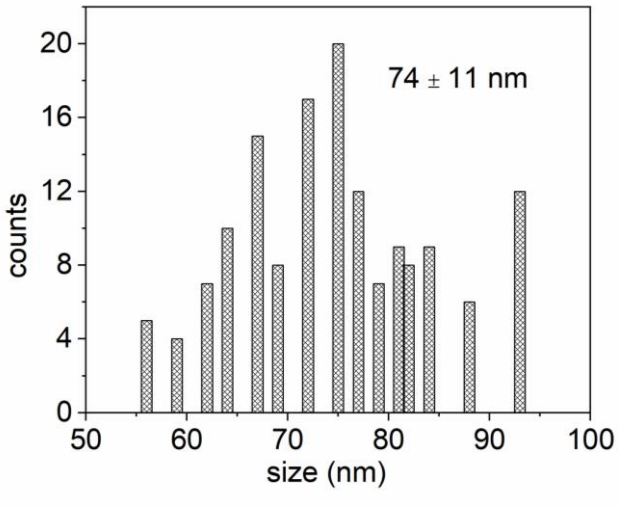

Fig. S2 Histogram showing the average dimensions of the nanoparticles of sodium niobate ($NaNbO_3$) disordered pyrochlore. Mean size of the nanoparticles was 74 nm as measured from 150 independent nanoparticles. The variance of 11 nm is reported as one standard deviation from the calculated mean value.

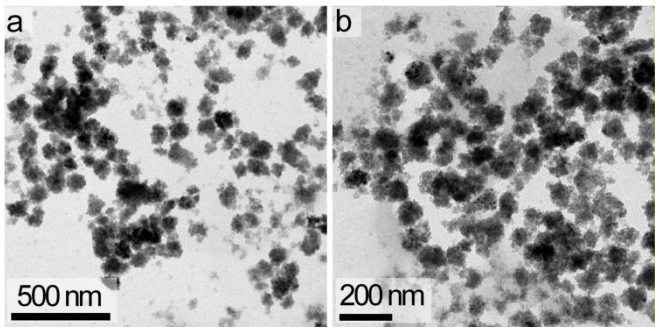

Fig. S3 Transmission electron microscopy (TEM) of the product obtained after a reaction time of 3 d.

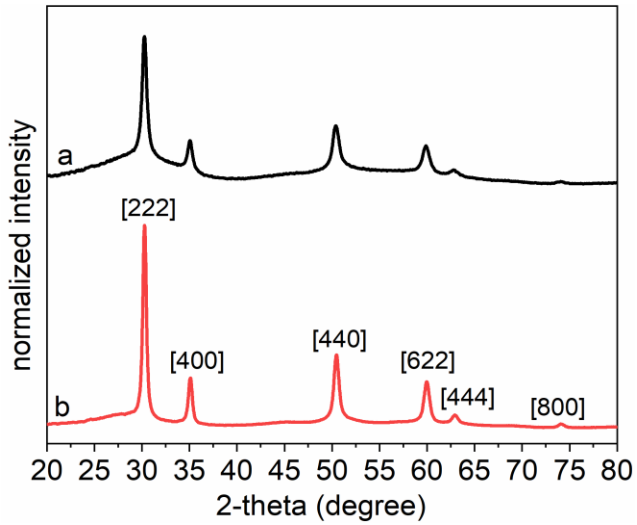

Fig. S4 Powder X-ray diffraction (XRD) patterns the products obtained after a reaction time of: (a) 3 d and (b) 4 d.

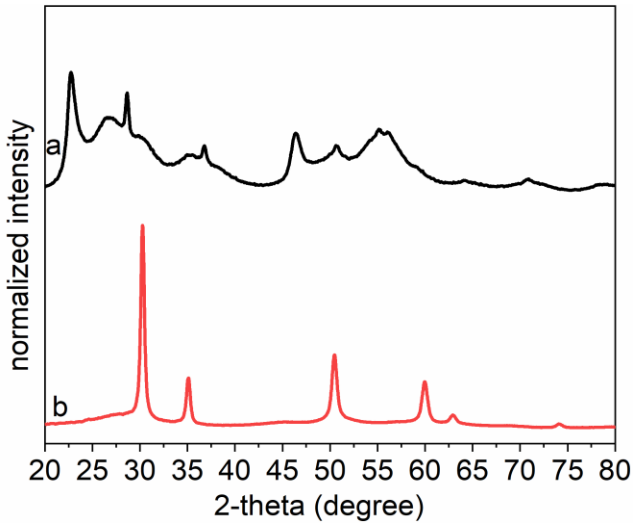

Fig. S5 Powder X-ray diffraction (XRD) patterns the products obtained after a reaction time of 4 d using: (a) SDS and (b) triethylamine.

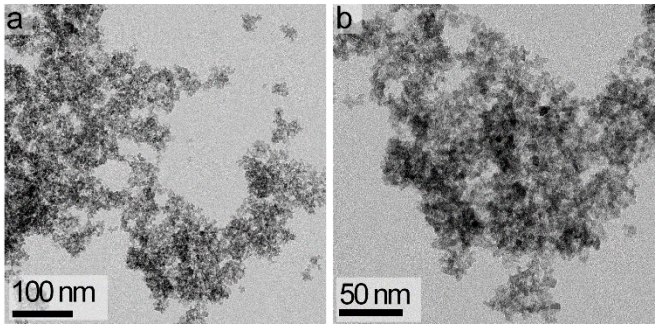

Fig. S6 Transmission electron microscopy (TEM) of the product obtained after a reaction time of 4 d using SDS.

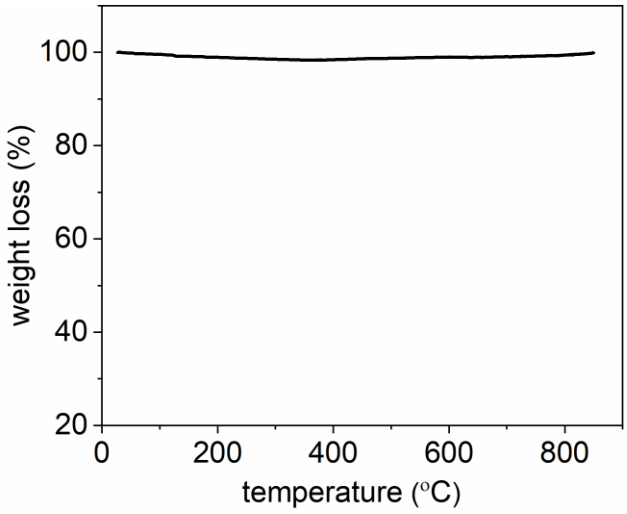

Fig. S7 Thermogravimetric analysis (TGA) of the nanoparticles of a $NaNbO_3$ disordered pyrochlore when heated at a rate of 1 °C/min from 25 to 850 °C under an ambient atmosphere, which indicated the relative thermal stability of the product.

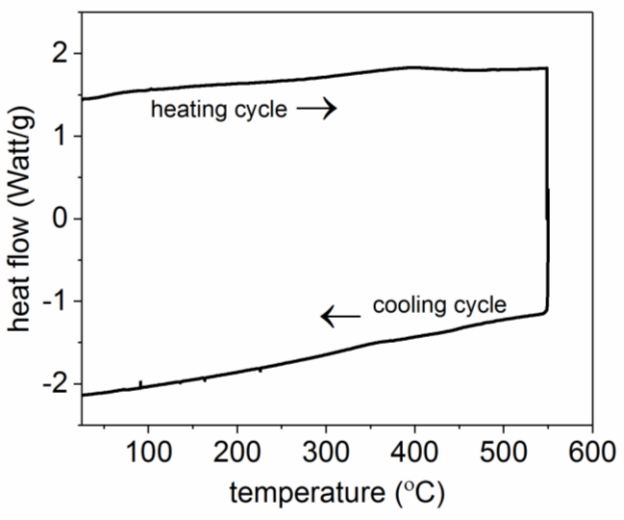

Fig. S8 Analysis by differential scanning calorimetry (DSC) of the $NaNbO_3$ disordered pyrochlore nanoparticles when heated and cooled between 25 to 550 °C. The DSC trace indicated the stability of the product over this temperature range by the absence of any phase transformations. The upper temperature was set to 550 °C due to the limitations of the DSC instrument.

Table S2. Average dimensions of the crystallites as estimated by Scherrer analyses of the XRD data collected at the specified temperatures for defect-fluorite pyrochlore nanoparticles of $NaNbO_3$.

temperature (°C)	peak position [2-theta (degree)]	average crystallite size (nm)
30	29.9	27.6
200	29.9	27.2
300	29.9	26.6
350	29.9	25.9
400	29.9	26.2
450	29.9	26.3
500	29.9	25.5
600	29.2	23.6
700	29.2	18.8
800	29.2	19.0

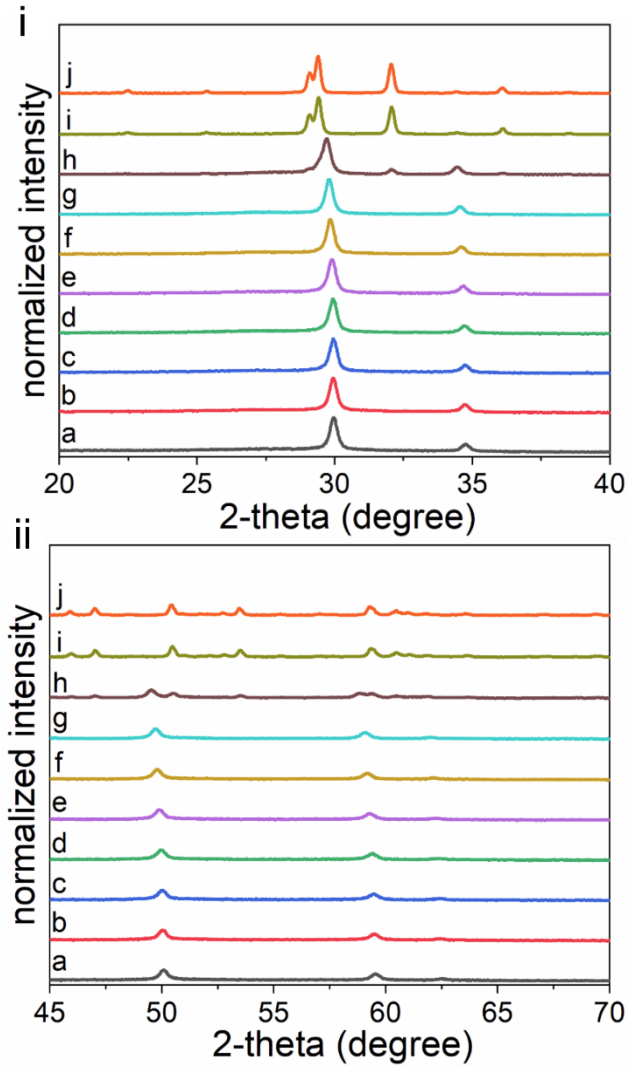

Fig. S9 Temperature dependent XRD patterns of $NaNbO_3$ nanoparticles at 2-theta values from: (i) 20° to 40°; and (ii) 45° to 70°. These diffraction patterns were obtained after heating the sample to various set-point temperatures: (a) 30 °C; (b) 200 °C; (c) 300 °C; (d) 350 °C; (e) 400 °C; (f) 450 °C; (g) 500 °C; (h) 600 °C; (i) 700 °C; and (j) 800 °C.

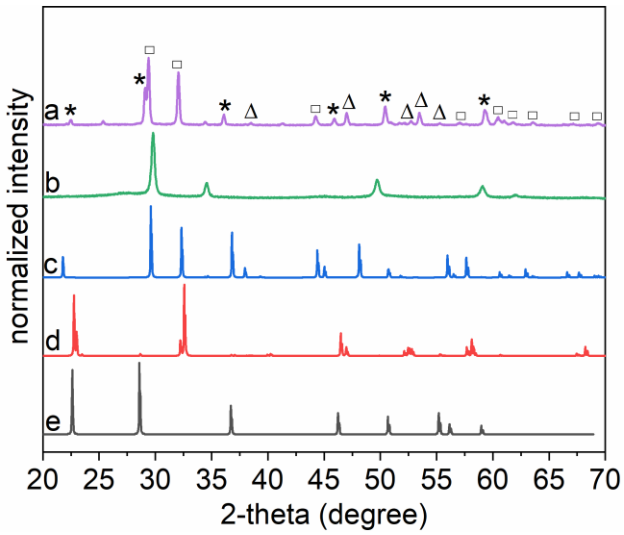

Fig. S10 X-ray diffraction patterns of defect-fluorite pyrochlore nanoparticles of $NaNbO_3$ after calcination of the product at (a) 800 ^oC and (b) 500 ^oC. Also included are the reported XRD patterns of: (c) a rhombohedral $NaNbO_3$ product corresponding to JCPDS No. 006-0173 [□]; (d) an orthorhombic $NaNbO_3$ product corresponding to JCPDS No. 077-0261 [Δ]; and (e) a pseudo-hexagonal Nb_2O_5 product corresponding to JCPDS No. 028-0317 [★].

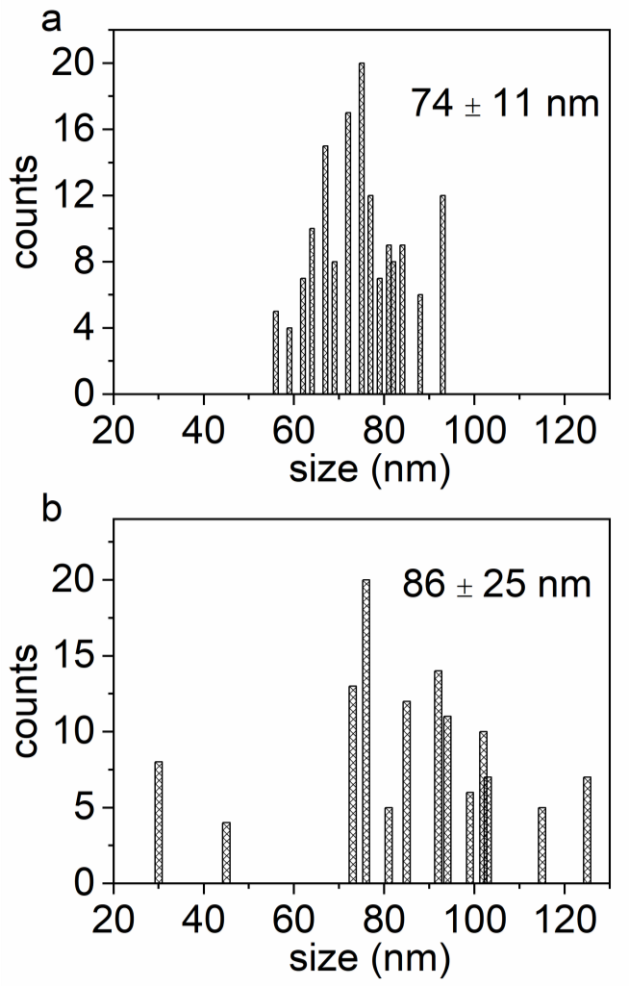

Fig. S11 Histograms showing a comparison of the average dimensions of the $NaNbO_3$ nanoparticles: (a) before neutron exposure; and (b) after neutron irradiation for 1 h. Mean size of the nanoparticles after neutron irradiation was 86 nm as measured from 122 independent nanoparticles. The variance of 25 nm is reported as one standard deviation from the calculated mean value.

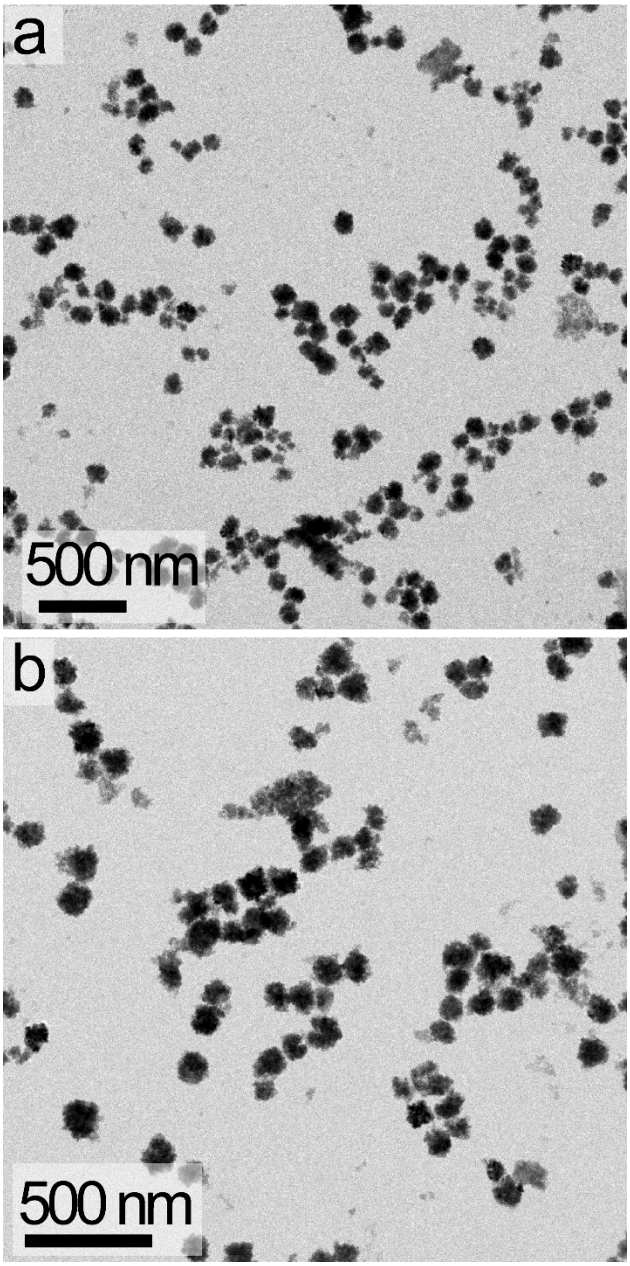

Fig. S12 Transmission electron microscopy (TEM) analysis of disordered pyrochlore $NaNbO_3$ nanoparticles after their exposure to neutron radiation for 1 h. The presence of smaller nanoparticles in the TEM images indicated the fragmentation of some M–O bonds following their exposure to energetic neutrons.

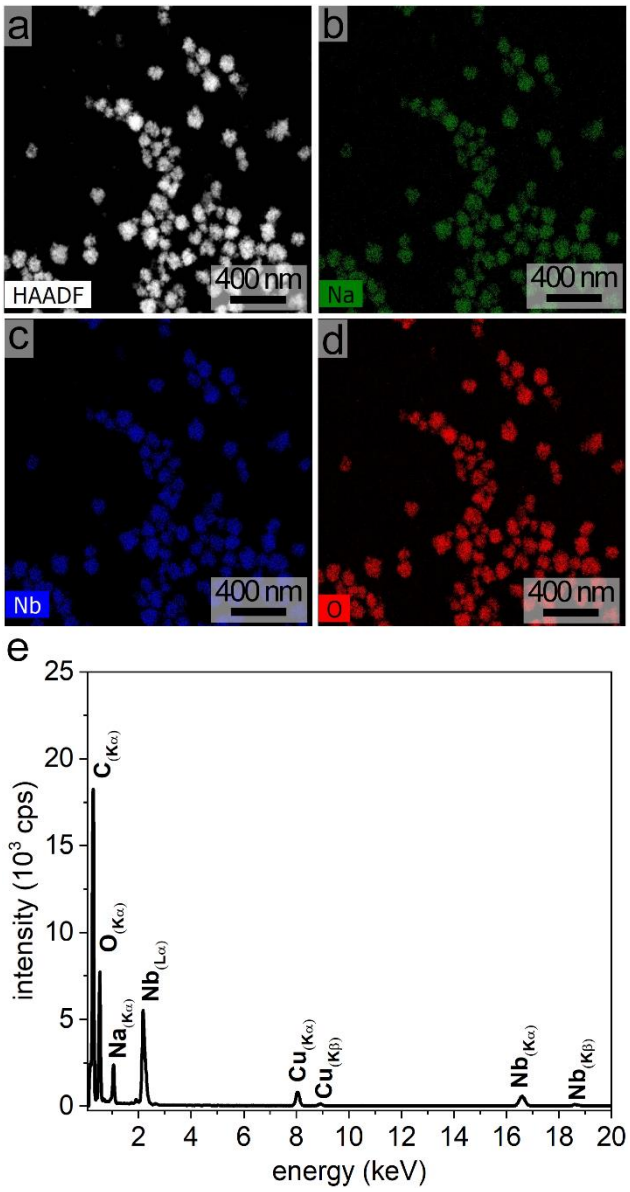

Fig. S13 Further TEM and energy dispersed X-ray spectroscopy (EDS) analysis of defect-fluorite pyrochlore nanoparticles of $NaNbO_3$ after radiation exposure. (a) A high-angle annular dark-field (HAADF) scanning TEM (STEM) image, and corresponding elemental maps obtained by EDS for: (b) Na; (c) Nb; and (d) O. (e) An EDS spectrum corresponding to the nanoparticles further indicating the presence of Na, Nb and O in the product. The copper (Cu) signals in the spectrum originated from the Cu TEM grid supporting the sample.